





Binding ability of Delta and Omicron towards the angiotensin-converting enzyme 2 receptor and antibodies: a computational study

Quoc-Thai Nguyen^a , Tan Thanh Mai^a, Lam-Truong Tuong^a, Thi-Thao-Nhung Nguyen^b, Thanh-Phuong Vo^b,
Dac-Nhan Nguyen^b, Cong-Thanh Phan-Van^a, Dieu-Thuong Thi Trinh^c, Van-Thanh Tran^a, and Khac-Minh Thai^b 

^aFaculty of Pharmacy, University of Medicine and Pharmacy at Ho Chi Minh City, Ho Chi Minh City, Vietnam; ^bUniversity of Health Sciences, Vietnam National University Ho Chi Minh City, Ho Chi Minh City, Vietnam; ^cTraditional Medicine Administration, Ministry of Health, Ha Noi City, Vietnam

ABSTRACT

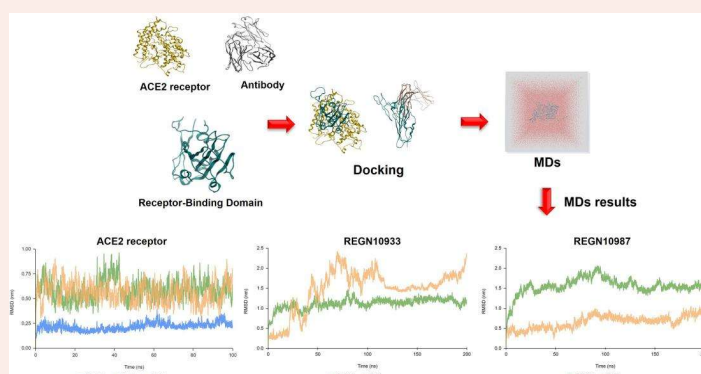
The COVID-19 pandemic posed a threat to global society. Delta and Omicron are concerning variants due to the risk of increasing human-to-human transmissibility and immune evasion. This study aims to evaluate the binding ability of these variants toward the angiotensin-converting enzyme 2 receptor and antibodies using a computational approach. The receptor-binding domain (RBD) of the two variants was created by CHARMM-GUI and then docked to the hACE2 receptor and two antibodies (REGN10933 and REGN10987). These complexes were also subjected to molecular dynamics simulation within 100 ns. As a result, the two variants, Omicron and Delta, exhibited stronger interaction with the hACE2 receptor than the wild type. The mutations in the RBD region also facilitated the virus's escape from antibody neutralization.

ARTICLE HISTORY

Received 24 November 2023
Accepted 31 August 2024

KEYWORDS

SARS-CoV-2; spike protein; receptor-binding domain; COVID-19; dynamics simulation



Introduction

The COVID-19 pandemic emerged from Wuhan, China, in early 2020. To date, the World Health Organization (WHO) has reported that the global number of COVID-19 cases exceeds 775 million (World Health Organization, 2024a), with the total number of deaths surpassing 7 million (World Health Organization, 2024b). SARS-CoV-2 is a member of the human coronavirus family, sharing a similar structure with SARS-CoV and MERS-CoV (Cui et al., 2019). According to the WHO, current variants of coronavirus are divided into two main groups: Variants of Concern (VOC) and Variants of Interest (VOI). Variants in the VOC group include Alpha (B.1.1.7), Beta (B.1.351), Gamma (P.1), and Delta (B.1.617.2). The difference in transmissibility and virulence depends on mutative strains (*Variants of the Virus*, 2023). In late November 2021, the WHO classified the Omicron variant

(B.1.1.529) as a VOC (*Tracking SARS-CoV-2 Variants*, n.d.). Additionally, the Delta and Omicron variants have had a significant public health impact, altering disease transmissibility and potentially reducing the efficacy of prevention methods (Chavda et al., 2022; Dhama et al., 2023). The high infectivity of SARS-CoV-2 can be attributed to its increased binding efficiency to ACE2 and the alternation of the virus at the binding site of antibodies, leading to the antibody evasion (Liu et al., 2022; Wrapp et al., 2020). Therefore, this study aims to assess the binding ability of hACE2 and antibodies towards variants by docking approach to evaluate the pathogenicity and transmission of these variants.

The SARS-CoV-2 structure includes spike protein, membrane protein, envelope protein, nucleocapsid protein, and hemagglutinin (HA) (Zhou et al., 2020). SARS-CoV-2 infects humans by initially binding the surface spike protein to the human angiotensin-converting enzyme 2 (hACE2) receptor

(Hoffmann et al., 2020). Therefore, the spike protein is a popular target for vaccine development and therapeutic interventions (Jackson et al., 2022; Premkumar et al., 2020; Singh et al., 2021; Yang et al., 2020). The spike protein is a glycoprotein consisting of an S1 subunit and an S2 subunit. The N-terminal domain and a receptor-binding domain (RBD) in the S1 subunit play a vital role in interacting between virus and host cells, as well as neutralizing antibodies (Walls et al., 2020). Meanwhile, the HR-1 and HR-2 regions in the S2 subunit are responsible for the membrane fusion.

The spike protein structure of Delta variant was identified to have eight mutations. These mutations affect different regions: T19R, G142D, Δ 156–157, and R158G in the N-terminal domain (NTD), two mutations in the receptor-binding domain (RBD) (L452R and T478K), one in the furin cleavage site (P681R), and another in the S2 area (D950N) (Ecdc, 2022). It's worth noting that mutations in the receptor-binding domain of the SARS-CoV-2 spike protein, such as L452R and P681R, have been associated with increased transmissibility in the Delta variant. The Omicron variant (B.1.1.529) has 3 deletions (Δ 69–70, Δ 143–145, Δ 211), 1 insertions (ins214EPE), and 30 substitutions (A67V, T95I, G142D, L212I, G339D, S371L, S373P, S375F, K417N, N440K, G446S, S477N, T478K, E484A, Q493K, G496S, Q498R, N501Y, Y505H, T547K, D614G, H655Y, N679K, P681H, L1K96Y96, QF954K1H, N764K) related to the glycoprotein. Among these, the N501Y, K417N, and T478K mutations belonging to this variant are reported to have the dominant immune escape and infectivity to the Delta (Islam et al., 2022). In addition, the Omicron variant multiplies 70 times faster in the human bronchus than the Delta and original SARS-CoV-2 variants. This discovery may explain why Omicron spreads more rapidly than previous variants (Kumar et al., 2022). In contrast to the different effects of SARS-CoV-2, the hACE2 polymorphisms have no significant impact on infection and disease outcome (Gómez et al., 2020; Möhlendick et al., 2021).

Wang et al. conducted an in-depth analysis to determine which amino acids play a critical role in the formation of the complex between the virus and the hACE2 receptor (Wang et al., 2020). A network of hydrogen bonds and salt bridges is formed by a collection of hydrophilic amino acids, which create significant polar contacts. These polar contacts include interactions between A475, N487, E484, Y453 of SARS-CoV-2 RBD and S19, Q24, K31, H34 of hACE2 receptor, respectively. The residue K417 in the RBD subdomain is involved in an ionic interaction with residue D30 of hACE2. The loop α 1'/ β 1' and β 2'/ η 1' loops in RBD position residues (G446, Y449, G496, Q498, T500, and G502) near hACE2 amino acids D38, Y41, Q42, K353, and D355, thereby establishing a series of hydrogen bonds. Additional contacts between the virus and receptor are formed by SARS-CoV-2-CTD's Y489 and F486 against hACE2 residues F28, L79, M82, and Y83, creating a set of hydrophobic interactions at their interface.

Two main regions distinguish the binding interface between the hACE2 receptor and SARS-CoV-2. In the Omicron variant complex, the first region features hydrogen bonds between hACE2 and the RBD, including interactions from S19 to A475/N477, Q21 to N487, Y83 to Y489/N487, and H34 to Y453 (Han

et al., 2022). The residue F486 from Omicron's RBD is within a tight hydrophobic pocket at the interface, surrounded by hACE2 residues F28, L79, M82, and Y83. Conversely, in the Delta variant complex's first region, RBD residues A475, N487, Q493, Y453, and Y489 form hydrogen bonds with hACE2 residues S19, Q24, K31, H34, and Y83, respectively. A notable distinction is that in Omicron, the residue R493 forms a salt bridge with E35 of hACE2, while in Delta, the residue K417 engages in a salt bridge with D30 of hACE2. F486 from Delta's RBD performs a role similar to that in Omicron, fitting into the same hydrophobic pocket. In the second region of the Omicron variant complex, hydrogen bonds occur between hACE2 residues D38, Q42, Y41, and K353 and Omicron's RBD residues Y449, T500, and G502. Additionally, the residue D38 also forms a salt bridge with R498 of Omicron's RBD. In the Delta variant complex, hACE2 residues E37, D38, Y41, and K353 interact with RBD residues Y505, Y449, T600, and G496, respectively. Up to now, the treatment for SARS-CoV-2 includes using nucleotide analogs such as remdesivir to inhibit RNA-dependent RNA polymerase; immunosuppressive drugs or molecules acting on the immune response (corticoids, interferons, monoclonal antibodies against inflammatory cytokines, mesenchymal stem cells), and convalescent plasma therapy (Iacob & Iacob, 2020) for which, neutralizing antibodies (nAbs) targeting the RBD show a protective immunity against viral infections. During virus transmission, new variants having an amino acid replacement in spike protein sequences may affect the efficacy of neutralizing antibodies.

REGN10933 and REGN10987 are components of an antibody cocktail (REGN-COV2) against the SARS-CoV-2 spike protein, recently named casirivimab and imdevimab, respectively. SARS-CoV-2 variants such as Alpha, Beta, Gamma, Delta, and Omicron have increased infectivity and the ability to evade the human immune system (Cao et al., 2022; Planas et al., 2021). However, the combination of REGN10933 and REGN10987 antibodies has been shown to neutralize these variants (Tada et al., 2021; Takashita et al., 2022). Regeneron Pharmaceuticals researched and developed the REGN-COV2 antibody to treat patients with COVID-19 and prevent SARS-CoV-2 infection (Deeks, 2021). This antibody cocktail is being evaluated in four late-stage clinical trials, with continued recruitment of volunteers (Tuccori et al., 2020). The National Clinical Trial (NCT) numbers NCT4425629 and NCT4426695 are still investigating the efficacy of REGN-COV2 in Two-Phase 2/3 trials (Regeneron Pharmaceuticals, 2023). Besides, the NCT04452318 tests in the Phase 3 prevention trial. Moreover, the NCT04381936 evaluates REGN-COV2 in the open label Phase 3 at the University of Oxford (Mahase, 2020). The FDA recently approved emergency use authorization for the low-dose antibody REGN-COV2 in adults with mild to moderate COVID-19 who are at high risk for adverse outcomes (Regeneron Pharmaceuticals, 2020). Despite the recognized significance of REGN-COV2 in COVID-19 treatment, the detailed atomic-level structure and binding mechanism of REGN-COV2 antibodies to the RBD have not been thoroughly investigated. Therefore, comprehending the molecular mechanisms that govern the interactions of SARS-CoV-2 variants is crucial for identifying suitable and timely therapeutic interventions for COVID-19.

Protein-protein docking predicts the structure of a complex based on the structures of the individual proteins involved (S.-Y. Huang, 2014; Vakser, 2014). The molecular docking approach estimates binding capabilities across various conformations and ranks these conformations with a scoring function. Throughout docking results and dissociation constants (K_d), this study compared the binding affinities of variant complexes to those of wildtype complexes and evaluate the viral infectivity and escaping antibodies of Delta and Omicron based on the binding affinity of these variants with the hACE2 receptor and two antibodies (REGN10933 and REGN10987). Molecular dynamics simulations were employed to evaluate the stability of the complexes throughout the simulated time. The methodology flowchart involves 4 steps: (1) creating mutation in the RBD domain of Omicron and Delta, (2) docking these RBD structures to the hACE2 receptor and two antibodies (REGN10933 and REGN10987) for assessing the binding affinity, (3) calculating the Haddock score and dissociation constant (K_d) of these complexes, and (4) performing molecular dynamics simulation within 100 ns to evaluate the stability of protein-protein complexes.

Materials and methods

This study examines the ability of viral infectivity and antibody evasion of Omicron and Delta variants based on their binding affinity with the hACE2 receptor and two antibodies (REGN10933 and REGN10987). The research procedure is demonstrated in Figure 1. Firstly, the study created mutations in the receptor binding domain (RBD) of these variants via the CHARMM-GUI tool (Jo et al., 2008, 2014). Later, the study performed docking SARS-CoV-2 RBD (wild type and variants) to the hACE2 receptor and the neutralizing monoclonal antibodies (mAbs) using HADDOCK2.4 program (Van

Zundert et al., 2016) to calculate HADDOCK score. The PRODIGY was employed to predict the dissociation constant (K_d) and binding affinity (ΔG) (Xue et al., 2016). Afterward, the complexes of RBDs with hACE2 and mAbs were simulated by molecular dynamics (MD) by GROMACS 2020.4 software (GROMACS 2020.4 Manual, n.d.) within 100 ns. These findings were used to assess the viral infection, the resistance of SARS-CoV-2 variants to immunity, and vaccine effectiveness.

Creating in silico mutations in the RBD domain of SARS-CoV-2 variants

All the protein structures, including Crystal structure of SARS-CoV-2 spike receptor-binding domain bound with ACE2 (PDB ID: 6M0J) (Lan et al., 2020), Complex of SARS-CoV-2 receptor binding domain with the Fab fragments of two neutralizing antibodies REGN10933 and REGN10987 (PDB ID: 6XDG) (Hansen et al., 2020), were obtained from Protein Data Bank (<http://www.rcsb.org>) (Thai et al., 2015; V.-T. Tran et al., 2022; Tran-Nguyen et al., 2019). The RBD wildtype was mutated with multiple substitutions at pH 7.0 using *PDB reader & Manipulator* in CHARMM GUI web (Jo et al., 2008, 2014). The substitutions in the RBD of Omicron and Delta variants, as presented in Table 1, were then implemented using the *Mutation* option. Other parameters, including protonation state and disulfide bonds, were automatically detected by the *PDB Reader & Manipulator* (Park et al., 2023) and set to default. These structures were then energy-minimized using the QuickPrep tool in MOE 2015.10 software in preparation for the molecular docking step.

Molecular docking

The HADDOCK 2.4 server (Van Zundert et al., 2016) was used to evaluate the binding affinity between wild-type and SARS-

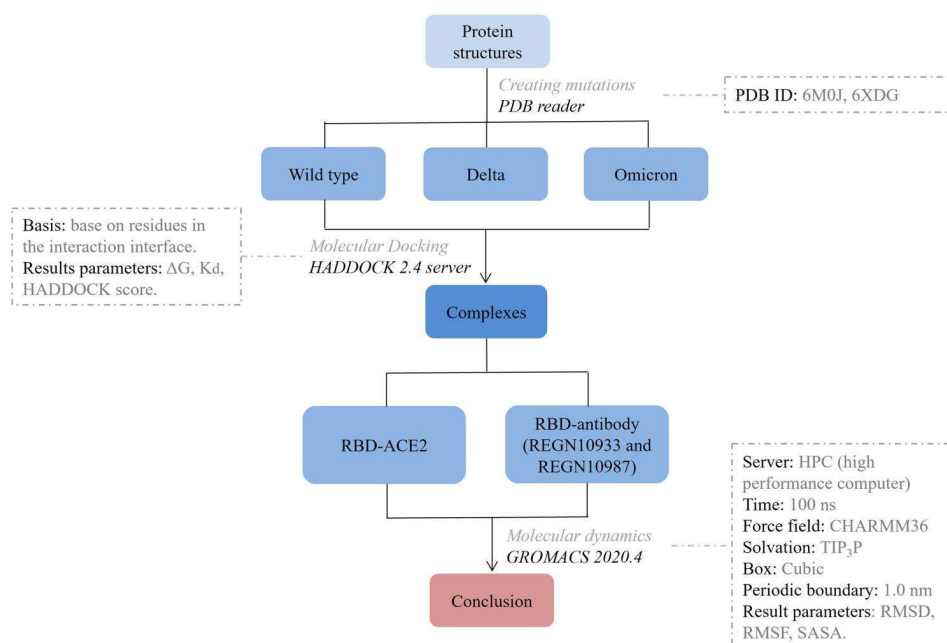


Figure 1. Summary of the research process.

Table 1. Substitution mutations in the receptor-binding domain (RBD) domain of Omicron and Delta variants.

SARS-CoV-2 variants	Substitution mutations in the RBD domain
Omicron	G339D, S371L, S373P, S375F, K417N, N440K, G446S, S477N, T478K, E484A, Q493K, G496S, Q498R, N501Y, Y505H, T547K
Delta	T478K, L452R

CoV-2 variants with the hACE2 receptor and neutralizing antibodies. The protein-protein docking was conducted according to the tutorial provided by HADDOCK 2.4 web server (Bonvinlab, 2022). The HADDOCK scoring function (Vangone et al., 2017) integrates a linear combination of multiple energy terms and buried surface area, with specific variations applied at different docking stages: rigid body (it0), semi-flexible refinement (it1), and explicit solvent refinement (water). Scoring is executed based on the weighted sum from these three terms, referred to as the HADDOCK score. The resulting clusters are analyzed and ranked based on the average HADDOCK score (HS) of their top four members.

$$\text{HADDOCKscore} - \text{it } 0 = 0.01 * E_{\text{vdw}} + 1.0 * E_{\text{elec}} + 1.0 * E_{\text{desol}} + 0.01 * E_{\text{air}} - 0.01 * \text{BSA} \quad (1)$$

$$\text{HADDOCKscore} - \text{it } 1 = 1.0 * E_{\text{vdw}} + 1.0 * E_{\text{elec}} + 1.0 * E_{\text{desol}} + 0.1 * E_{\text{air}} - 0.01 * \text{BSA} \quad (2)$$

$$\text{HADDOCKscore} - \text{water} = 1.0 * E_{\text{vdw}} + 0.2 * E_{\text{elec}} + 1.0 * E_{\text{desol}} + 0.1 * E_{\text{air}} \quad (3)$$

where E_{vdw} , E_{elec} , E_{desol} , E_{air} , and BSA denote van der Waals energy, electrostatic energy, desolvation energy, and air energy, the buried surface area, respectively.

A more negative HADDOCK score indicates a higher binding affinity of the complexes. Protein PDB files were prepared using PyMol software, removing water and non-bonded ions, and identifying residues in the interaction interface. These files were uploaded to HADDOCK web server to generate 10 clusters along with the HADDOCK score. After docking by the HADDOCK web server, the dissociation constant of the RBD-ACE2 and RBD-mAbs complexes predicted via the PRODIGY web server (Xue et al., 2016). The dissociation constant (K_d) is a vital parameter in calculating the binding strength of protein-protein complexes. The predictive model of PRODIGY is based on the number of interfacial contacts (ICs) of a protein-protein complex combined with properties of the non-interacting surfaces (NIS) to predict the binding affinity of protein-protein complexes.

Molecular dynamics simulations

Molecular dynamics simulations of RBD-ACE2 and RBD-antibody complexes were conducted using GROMACS 2020.4 software within 100 ns. The research employed the CHARMM36 force field (J. Huang et al., 2017), a cubic box with a periodic boundary condition of 1.0 nm, and the TIP3P solvent model (Boonstra et al., 2016). The system was neutralized with ion Na^+ and Cl^- at a concentration of 0.15 M, then energy minimized to lower than 10.0 kJ.mol^{-1} within

Table 2. Docking results of the wild type, Delta and Omicron variants with human angiotensin-converting enzyme 2 (hACE2) receptor.

	Wild type	Delta	Omicron
Haddock score	-141.8 ± 2.5	-151.7 ± 6.5	-157.7 ± 10.5
ΔG (kcal.mol^{-1})	-13.0	-13.7	-15.2
K_d (M)	3.1×10^{-10}	9.2×10^{-11}	7.5×10^{-12}

the maximum time of 100 ps. It was subsequently balanced at 300 K temperature and 0.978 atm (1 bar) for pressure. Temperature and pressure during simulation were maintained by the V-rescale and Parrinello–Rahman algorithms, respectively (Bussi et al., 2007; Parrinello & Rahman, 1981). The RMSD and RMSF values were calculated to evaluate the stability of the complexes. The study computed further the solvent accessible surface area (SASA) of each residue in the protein structure (Le et al., 2020, 2021; Mai et al., 2022; Phan et al., 2024; Phan et al., 2023; Phan et al., 2023; Q.-H. Tran et al., 2023; T.-T.-N. Tran et al., 2023).

The root mean square deviation (RMSD) is a key metric used to assess the stability of atoms in simulations, providing insight into the stability of protein-protein complexes. A complex is considered stable when the RMSD value is below 2 Å (Xiao et al., 2018). Additionally, the root mean square fluctuation (RMSF) value is employed to measure the flexibility of each amino acid's position or the degree of fluctuation of specific amino acids during simulations. An RMSF value greater than 2 Å indicates amino acid flexibility (Sundar et al., 2019). On the other hand, the solvent accessible surface area (SASA) value serves as a metric for evaluating protein stability and folding. A smaller SASA value indicates greater protein stability (Durham et al., 2009).

Results

Docking results

Binding ability toward ACE2 receptor

The docking results of RBD-ACE2 complexes of the wild type, Delta, and Omicron variants are presented in Table 2. The Haddock score of Omicron was more negative than that of the Delta and wild-type, with $-157.7 \pm 10.5 \text{ kcal.mol}^{-1}$, $-151.7 \pm 6.5 \text{ kcal.mol}^{-1}$ and $-141.8 \pm 2.5 \text{ kcal.mol}^{-1}$, respectively. This indicates that the Omicron may significantly increase the ACE2-binding affinity and thus enhance the viral infectivity. A much higher binding affinity of the Delta compared to the wild type is also demonstrated by the Haddock score. The dissociation constant (K_d) of RBD-Omicron to ACE2 was $7.5 \times 10^{-12} \text{ M}$ at 25.0°C ($\Delta G = -15.2 \text{ kcal.mol}^{-1}$), which was 41-times smaller than the original form. The Delta had the dissociation constant (K_d) slightly lower than the wild type, with $9.2 \times 10^{-11} \text{ M}$ and $3.1 \times 10^{-10} \text{ M}$, respectively. Therefore, the binding between the RBD domain and the

hACE2 receptor of the Omicron was predicted to be the most stable complex.

When comparing the interactions of the wild-type and hACE2 complex conducted by Haddock and that in crystal structure from PDB (Table 3 and Figure 2), the Haddock result showed the similarity of amino acid interactions between RBD and hACE2. This result indicated the accuracy and reproductivity of molecular docking approach in the RDB-hACE2 complex.

According to the Delta-hACE2 complex, despite the decrease in a number of interactions in the RBD region, consisting of G446, Y489, T500, N501, and Y505, the Haddock score of this complex is more negative than the wild-type complex. This higher binding ability of the Delta complex can be explained by the formation of 3 salt bridge interactions at K417, R455, and E484. The B.1.617.2 (Delta) variant is considered to be the most infectious of all variants and has become one of the most transmissible variants, for which, the L452R and T478K mutations play a significant role in the infectivity and transmissibility. The K417N mutation of the Delta plus variant contributes to more infections than the original form.

Regarding the Omicron-hACE2 complex, this complex has the additional interaction with substituted amino acids, including S477N, T478K, Q493K, and G496S. These interactions with higher Haddock score than WT complex play an important role in the tightly binding of Omicron and hACE2, thereby contributing to their great infectivity and transmissibility. The mutations K417N, T478K, N440K, S477N, and N501Y on Omicron are considered to contribute to the great infectivity and transmissibility (SARS-CoV-2 Variants of Concern as of 12 April, n.d.). In a study by Michael I Barton et al., the effects of individual RBD mutations found in new SARS-CoV-2 Alpha (B.1.1.7), Beta (B.1.351), and Gamma (P1) variants in terms of affinity and kinetics on the RBD/ACE2 interaction were evaluated. The study reported that both N501Y and S477N mutations had stronger binding affinity towards the hACE2

receptor and enhanced the SARS-CoV-2 infectivity (Barton et al., 2021). *In vivo* and *in vitro* tests of N501Y substitution in the B.1.1.7 (Alpha) variant on the hamster model revealed that replacing Asn with Tyr at residue 353 may increase binding affinity with the hACE2 receptor. Moreover, the study by Dixit Tandel et al. predicted N440K had higher binding affinity than the wild type (Tandel et al., 2021).

Antibody binding ability

Delta and Omicron variants have a lower binding ability with the REGN10933 antibody compared to the wild type, with docking scores of $-141.8 \pm 3.8 \text{ kcal.mol}^{-1}$ and $-137.0 \pm 5.4 \text{ kcal.mol}^{-1}$, respectively, compared to $-154.2 \pm 8.2 \text{ kcal.mol}^{-1}$. Moreover, these variants also tended to escape from the antibody with ΔG and K_d values much higher than that of the wild type (Table 4). Regarding the REGN10987 antibody, the binding of this antibody towards the Delta was considered unstable, with the Haddock score, ΔG , and K_d of $-99.4 \pm 1.9 \text{ kcal.mol}^{-1}$, $-13.5 \text{ kcal.mol}^{-1}$, and $1.2 \times 10^{-10} \text{ M}$, respectively. In contrast, the binding of this antibody with Omicron was even stronger than the wild-type complex, with the Haddock score of $-147.5 \pm 1.6 \text{ kcal.mol}^{-1}$. The interactions between the RBD and antibodies, as detailed in Tables 5 and 6 and illustrated in Figure 3, demonstrate that the formation of binding interactions at specific mutated amino acids significantly contributes to the enhanced binding affinity observed in the Omicron complexes relative to the wild-type complex. These critical mutations include N440K, S477N, Q493K, G496S, Q498R, N501Y, and Y505H.

Overall, Delta and Omicron variants were predicted to have a better binding capacity to the ACE2 than the wild type. According to the docking results of both the REGN10933 and REGN10987 antibodies, the binding of the Delta variant complex is looser than that of the wild type of complex, whereas Omicron has a contradictory result. Haddock scores are relatively similar, but compared to the wild type, REGN10987 is

Table 3. The interactions of the wild type, Delta and Omicron variants with human angiotensin-converting enzyme 2 (hACE2) receptor in the crystal structure and Haddock results.

Crystal structure (PDB 6M0J)		Haddock results					
		WT-hACE2 complex		Delta-hACE2 complex		Omicron-hACE2 complex	
RBD	hACE2	RBD	hACE2	RBD	hACE2	RBD	hACE2
K417	D30 (h-s)	K417	D30 (h-s)	K417	D30 (h-s)	R403	E35 (s)
G446	Q42 (h)	G446	Q42 (h)	Y449	D38 (h)	G416	K68 (h)
Y449	Q42 (h)	Y449	D38 (h)	R455	E35 (h-s)	Y453	E35 (h)
N487	Q24 (h)	A475	S19 (h)	A475	S19 (h)	N477	E329 (h)
	Y83 (h)						
	Q325 (h)						
	E329 (h)						
	N330 (h)						
Y489	Y83 (h)	E484	K31 (h-s)	E484	K31 (h-s)	K478	Q325 (h)
Q493	E35 (h)	N487	Q24 (h)	N487	Q24 (h)	N487	D355 (h)
	E37 (h)		Y83 (h)		Y83 (h)		
T500	Y41 (h)	Q493	K31 (h)	Q493	E35 (h)	K493	H34 (h)
			E35 (h)				
N501	Y41 (h)	G496	D38 (h)	G502	K353 (h)	S494	K31 (h)
			K353 (h)				
G502	K353 (h)	T500	Y41 (h)	Q506	Q325 (h)	S496	D30 (h)
Y505	E37 (h)	G502	K353 (h)			T500	Y83 (h)
	D38 (h)						
	R393 (h)						
		Q506	Q325 (h)				

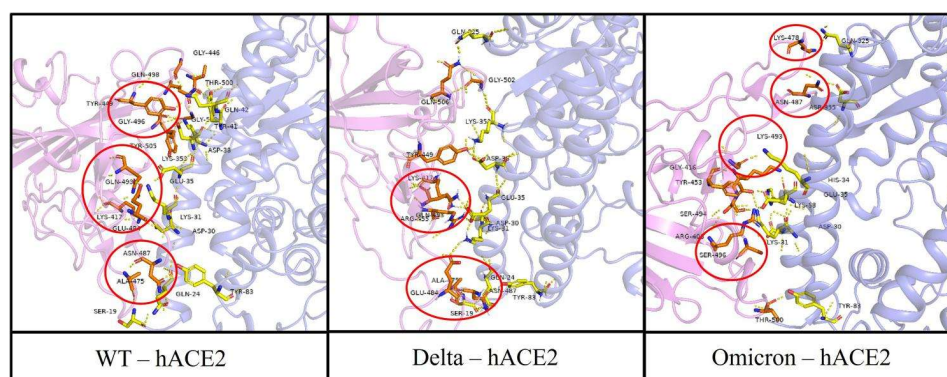


Figure 2. The interactions of the wild type, Delta and Omicron variants with human angiotensin-converting enzyme 2 (hACE2) receptor at the binding region.

Table 4. Docking results of the wild type, Delta and Omicron variants with antibodies (REGN10933, and REGN10987).

	REGN10933			REGN10987		
	Wild type	Delta	Omicron	Wild type	Delta	Omicron
Haddock score	-154.2 ± 8.2	-137.0 ± 5.4	-141.8 ± 3.8	-129.6 ± 1.1	-99.4 ± 1.9	-147.5 ± 1.6
ΔG (kcal.mol ⁻¹)	-12.9	-12.6	-13.4	-15.0	-13.5	-14.4
Kd (M)	3.5×10^{-10}	5.4×10^{-10}	1.6×10^{-10}	1.0×10^{-11}	1.2×10^{-10}	2.5×10^{-11}

Table 5. The interactions of the wild type, Delta and Omicron variants with the REGN10933 antibody in Haddock results.

WT-REGN10933 complex		Delta-REGN10933 complex		Omicron-REGN10933 complex	
RBD	REGN10933	RBD	REGN10933	RBD	REGN10933
K417	T316 (h)	R403	D245 (h-s)	R403	D1 (h-s)
Y449	T317 (h) S244 (h)	K417	T316 (h) T317 (h) M318 (h)	R408	D276 (h-s)
Y453	D245 (h)	R455	R314 (h) G315 (h)	T415	K279 (h)
A475	Y32 (h)	A475	Y32 (h)	L455	Y273 (h)
E484	Y247 (h) T266 (h) T271 (h)	S477	D92 (h)	Y473	S270 (h)
N487	R314 (h)	K478	N93 (h)	A475	Y247 (h)
Y489	R314 (h)	E484	Y267 (h) S268 (h) S270 (h)	N477	D245 (h)
S494	D245 (h)	F486	Y273 (a)	F486	T316 (a)
		N487	D92 (h)	K493	D92 (h-s)
		Q493	R314 (h) S244 (h) D245 (h)	R498	D28 (h-s) T36 (h)
		Y505	G240	H505	D1 (h)

Table 6. The interactions of the wild type, Delta and Omicron variants with the REGN10987 antibody in Haddock results.

Haddock results					
WT-REGN10987 complex		Delta-REGN10987 complex		Omicron-REGN10987 complex	
RBD	REGN10987	RBD	REGN10987	RBD	REGN10987
R346	T730 (h)	N440	D480 (h)	N437	Y479 (h)
N439	Y479 (h)	V445	Y485 (a)	K440	Y479 (h) D480 (h-s)
S443	Y479 (h)	G446	S731 (h)	V445	Y485 (h)
K444	G525 (h) G529 (h)	Q498	Y531 (h)	S496	D530 (h)
G446	S526 (h) G529 (h) D530 (h)	P499	A459 (h) S478 (h)	R498	T730 (h)
N448	D530 (h)	T500	A459 (h)	P499	S478 (h)
Y449	D530 (h)	G502	N457 (h)	T500	Y461 (h)
		V503	N457 (h)	Y501	D530 (h)
				V503	N457 (h)
				G504	D527 (h)
				Q506	Y479 (h)

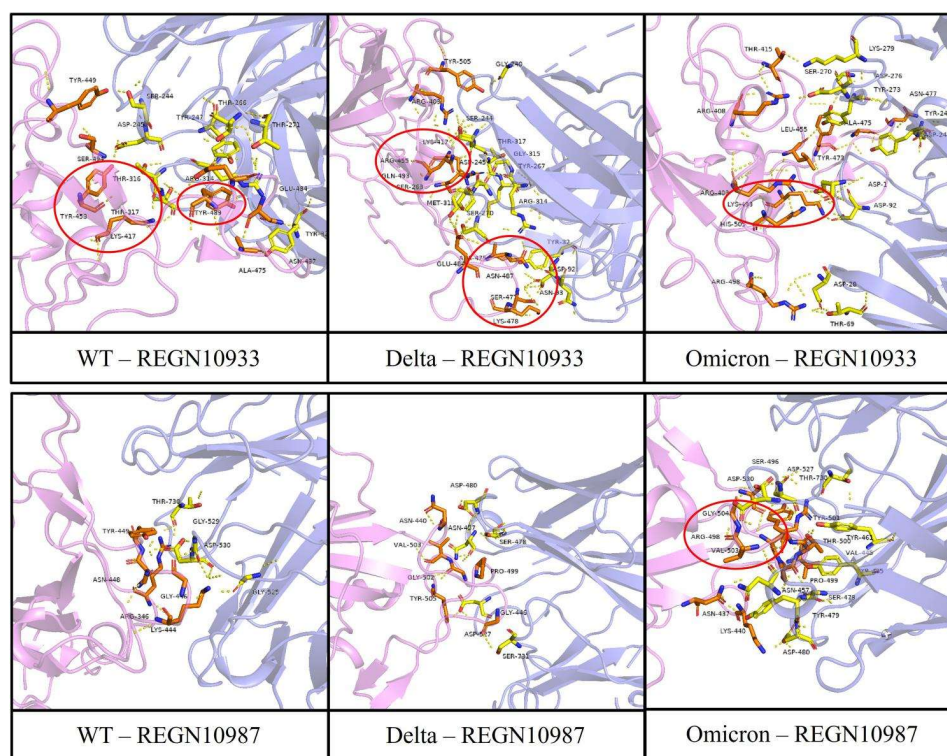


Figure 3. The interactions of the wild type, Delta and Omicron variants with antibodies (REGN10933 and REGN10987) at the binding region.

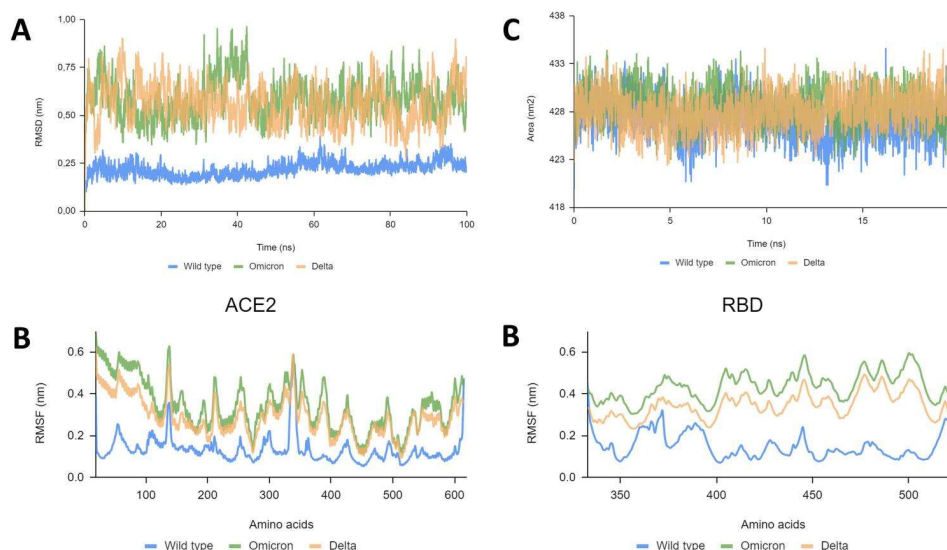


Figure 4. Analysis of RMSD, RMSF and SASA of the RBD – hACE2 complexes over the 100 ns simulation. (A) Root-mean-square deviation (RMSD) of the backbone, (B) Solvent accessible surface area (SASA), (C) Root-mean-square fluctuation (RMSF) of hACE2, and (D) Root-mean-square fluctuation (RMSF) of RBD.

more tightly bound while REGN10933 is more loosely bound for Omicron. Delta could escape immunity with two antibodies due to the loose binding of these complexes. On the other hand, the Omicron could bind strongly to REGN10987, suggesting an active against Omicron of this antibody.

Molecular dynamics simulation (MDs)

RBD-ACE2 complexes of the wild type, Delta, and Omicron

During the 100 ns simulation, the RMSD values of the RBDWT-ACE2 complex fluctuated between 0.15–0.40 nm. In the first 50 ns, the RMSD values of the RBDWT-ACE2 complex

were around 0.2 nm, then reached 0.4 nm at 70 ns and remained unchanged during the last period. Meanwhile, Delta and Omicron variant had higher RMSD values than the wildtype, and the omicron complex even fluctuated unsustainably in the first 50 ns with a peak of 1.0 nm at 40 ns (Figure 4A). In terms of the flexibility of amino acids in the binding site, RMSF value of the wide-type complex ranged within 0.1–0.3 nm, while both delta and omicron complexes gained the RMSF values than the wild type, at 0.1–0.6 nm and 0.1–0.5 nm, respectively (Figure 4C,D). This value indicated that there was an unstable binding between these variants and the hACE2 receptor. There was no significant

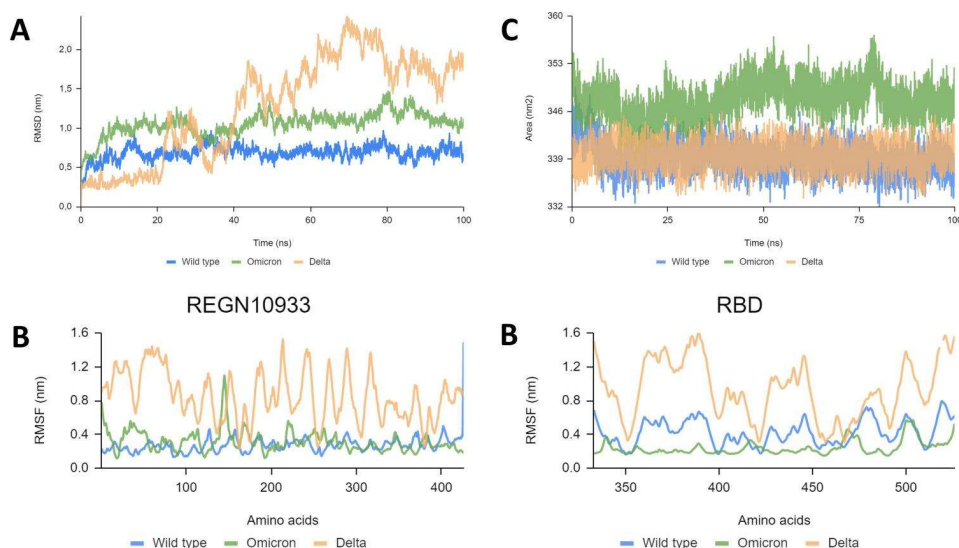


Figure 5. Analysis of RMSD, RMSF and SASA of the RBD – REGN10933 complexes over the 100 ns simulation. (A) Root-mean-square deviation (RMSD) of the backbone, (B) Solvent accessible surface area (SASA), (C) Root-mean-square fluctuation (RMSF) of REGN10933, and (D) Root-mean-square fluctuation (RMSF) of RBD.

difference in solvent accessible surface area (SASA) figures, where the three complexes had a similar trend between 420 and 435 nm² (Figure 4B).

Binding to the REGN10933 antibody

The RMSD value of the RBD_{WT}–REGN10933 complex stably fluctuated within 0.5–1.0 nm throughout the simulation time. Omicron variants also had a stable oscillation with the RMSD value between 0.8 and 1.5 nm. Whereas the fluctuation of the RBD_{Delta}–REGN10933 complex considerably increased from 0.3 to 2.4 nm in the first 80 ns and was more stable with the RMSD value under 2.0 nm (Figure 5A). The flexibility of the WT and variants of amino acids was shown as the RMSF value (Figure 5C,D). Corresponding to the RMSD values, the RMSF values of the WT and Omicron variant are stable throughout the simulation time at 0.2–0.6 nm, and Delta variant had more substantial flexibility for both RBD and antibody within 0.2–1.5 nm. Moreover, the amino acids of the RBD region of the Omicron variant fluctuated more stable than the wild type, which leads to the tightly binding of the Omicron variant toward the REGN10933 antibody and the remaining impactation of the REGN10933 antibody on the Omicron variant. Regarding the SASA values (Figure 5B), there was no significant difference between the wild type and the variants, with the SASA value ranging from 420 to 438 nm². Especially, the Omicron variants had a gradual decrease at 420–430 nm² after 50 ns, increasing the protein stability in the binding process.

Binding to the REGN10987 antibody

The RMSD values of the WT and the Delta are relatively stabilized. At the same time, the vibration amplitude of the Omicron was unstable because the Omicron's RMSD value increased rapidly from 0.2 to 2.2 nm (Figure 6A). In the first 40 ns, the RMSD values of the WT and the Delta overlapped at 0.25–0.65 nm. However, the WT's value rose quickly from 40 to 75 ns while the Delta's value remained stable.

The RMSF values of the critical residues in the RBD region (Figure 6C,D) were more stable in Delta and Omicron than in the WT. Concerning the REGN10933 antibody, the SASA values of WT and Delta (327–345 nm²) were lower than those of the Omicron variant (338–353 nm²). These results showed that the REGN10987–WT and REGN10987–Delta complexes were more stable than the REGN10987–Omicron (Figure 6B).

Extend MDs complexes between Delta and Omicron variants with antibodies

During the 100 ns simulation period, the complexes of the wildtype and hACE2 exhibited stability for most of the simulation time, except for higher fluctuations observed in the antibodies with variant complexes, particularly Delta–REGN10933 and Omicron–REGN10987. We extended the simulation time to 200 ns for the variants with antibodies to further assess the molecular dynamics results of these complexes.

RBD–REGN10933 complexes of the Delta, and Omicron variants

After extending the simulation duration of RBD–REGN10933 antibodies from 100 ns to 200 ns, the RMSD values of the variants exhibited varying degrees of stability. Notably, the RMSD of the Omicron variant remained stable during the last 100 ns, whereas the RMSD of the Delta variant showed a similar trend from 120 ns to 170 ns and witnessed a surge increase of 1.0 nm after that (Figure 7A). Furthermore, the RMSF values of the Delta variant in both the receptor-binding domain (RBD) and the antibody remained less stable than the Omicron variant (Figure 7C,D). According to the SASA value, Omicron complex during 200 ns simulation witnessed more stable than that of 100 ns, and Delta complex has no significant change (Figure 7B).

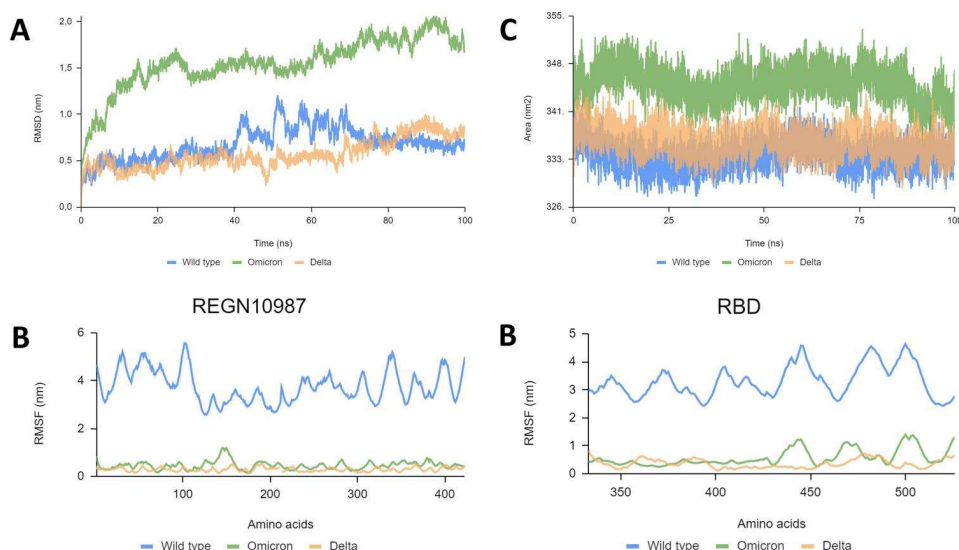


Figure 6. Analysis of RMSD, RMSF and SASA of the RBD – REGN10987 complexes over the 100 ns simulation. (A) Root-mean-square deviation (RMSD) of the backbone, (B) Solvent accessible surface area (SASA), (C) Root-mean-square fluctuation (RMSF) of REGN10987, and (D) Root-mean-square fluctuation (RMSF) of RBD.

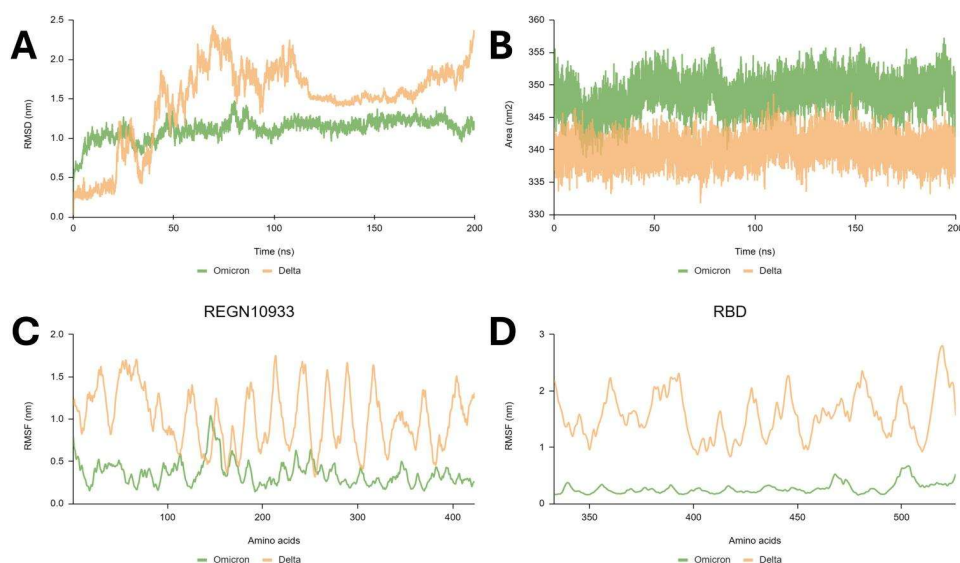


Figure 7. Analysis of RMSD, RMSF and SASA of the RBD – REGN10933 complexes over the 200 ns simulation. (A) Root-mean-square deviation (RMSD) of the backbone, (B) Solvent accessible surface area (SASA), (C) Root-mean-square fluctuation (RMSF) of REGN10933, and (D) Root-mean-square fluctuation (RMSF) of RBD.

RBD-REGN10987 complexes of the Delta, and Omicron variants

The RMSD values of both the Delta and Omicron variants exhibited stability from 100 ns to 200 ns, due to the unstable fluctuation in the first 100 ns (Figure 8A). Notably, despite this stabilization, the RMSD value of Delta remained more consistent compared to that of Omicron. Furthermore, an analysis of the RMSF (Figure 8C,D) in critical residues revealed a robust fluctuation in Omicron compared to Delta, observed in both the antibody and the RBD regions. Additionally, the SASA analysis (Figure 8B) showed that the SASA value of Omicron remained higher than that of Delta when interacting with both REGN10987 and REGN10933. This suggests that while REGN10987 continues to exhibit efficacy against the Delta variant, it appears ineffective against the Omicron variant, indicating potential differences in the binding dynamics and therapeutic implications between the two variants.

Discussion

Our investigation employed molecular docking and molecular dynamics simulations to explore the binding affinity of the Delta and Omicron variants to the hACE2 receptor, assessing their implications for viral infectivity and the neutralization potential of REGN-COV2 antibodies. In this study, the haddock results demonstrate that the Omicron and Delta variants exhibit an increased the binding affinity with the hACE2 receptor compared to the wild type, particularly the Omicron variant, which displays a HADDOCK score of $(-157.7 \pm 10.5 \text{ kcal.mol}^{-1})$ and a dissociation constant (K_d) of $(7.5 \times 10^{-12} \text{ M})$. However, these variants show more unsustainable fluctuations throughout the MD simulation with hACE2 receptor than the wild type. The transmissibility of Omicron in South Africa and the UK are >3.0 -fold and >5.6 -fold than that of Delta, suggesting that Omicron potentially

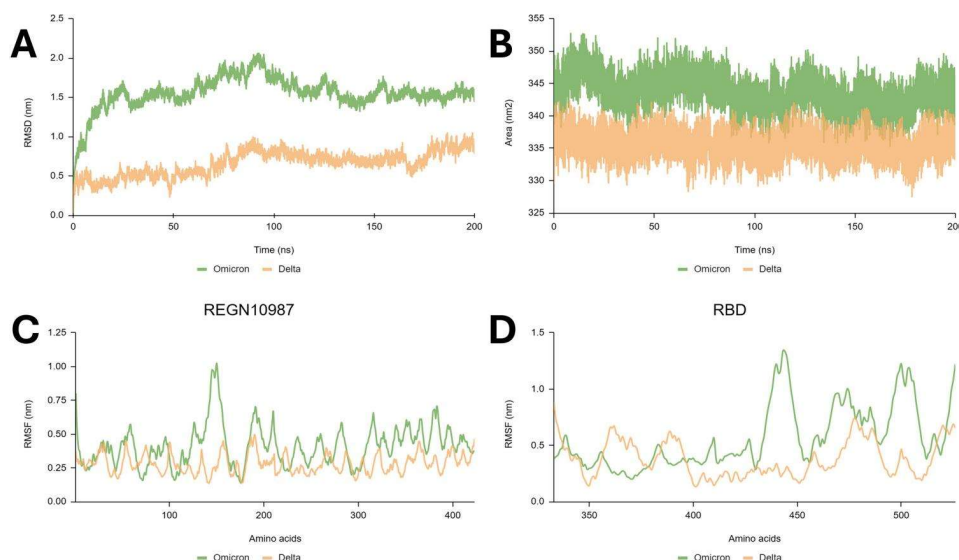


Figure 8. Analysis of RMSD, RMSF and SASA of the RBD – REGN10987 complexes over the 200 ns simulation. (A) Root-mean-square deviation (RMSD) of the backbone, (B) Solvent accessible surface area (SASA), (C) Root-mean-square fluctuation (RMSF) of REGN10987, and (D) Root-mean-square fluctuation (RMSF) of RBD.

outperforms Delta (Suzuki et al., 2022). A recent study by Kei Sato et al. on the Omicron variant indicates that Omicron might exhibit increased transmissibility and attenuated pathogenicity compared to the wild type based on cell culture experiments and hamster models. Therefore, both results of this study and the study by Kei Sato et al. indicate the Omicron have a high binding affinity with hACE2 as well as enhanced viral infectivity. The heightened affinity observed between the Delta and Omicron variants and the hACE2 receptor suggests a facilitated viral entry process. This may result in heightened viral replication within host cells and subsequently contribute to increased viral loads and augmented transmissibility. An in-depth comprehension of the molecular mechanisms underlying this enhanced binding affinity is crucial for elucidating viral infection pathways. Such insights not only improve our understanding of the infective potential of these variants but also lay the groundwork for the development of targeted therapeutic interventions aimed at mitigating the risk of severe outcomes, including mortality, in affected individuals.

Regarding the MD results of this study, all wildtype complexes achieved stable oscillation states after 10 ns and maintained this stability until the end of the period. All hACE2 complexes exhibited a similar pattern. Consequently, the MD results for these complexes can be used to analyze their binding over the simulation time. The exception to the 100 ns simulation time was the complexes between variants and antibodies, which underwent higher fluctuations. To obtain more accurate MD results, we extended the simulation time to 200 ns. The extended MD results showed that the oscillations from 100 ns to 200 ns remained within a similar fluctuation range as the first 100 ns, except for the Delta-REGN10933 complex, which became more stable than during the first 100 ns but gradually increased in fluctuation to reach values similar to those observed in the first 100 ns. These results indicate that the 100 ns simulation time is appropriate for capturing the dynamics of these proteins and can be applied to other studies involving these proteins,

such as protein-ligand complexes relating to SAR-CoV-2 and its variants (Bhardwaj et al., 2021; Sharma et al., 2021; Singh & Purohit, 2024).

The results regarding the REGN10933 antibody reveal an increased binding ability with the Omicron variant and a decreased binding ability with the Delta variant. Concerning the REGN10987 antibody, the Omicron variant binds more tightly to this antibody and the Delta variant binds more loosely to this antibody than the wild type with the stable binding process. According to Planas et al., the REGN-COV2 can be against the Delta variant (Planas et al., 2021). Emi Takashita et al. recently assessed the neutralizing activities of monoclonal anti-bodies against hCoV-19 variants. The REGN10987 (marketed as imdevimab) and the REGN10933 (marketed as casirivimab) also inhibited the Delta variant. Besides, imdevimab had lost activity against Omicron, while casirivimab still neutralized the Omicron variant (Takashita et al., 2022). These findings suggest that the combination of two antibodies, such as REGN10933 and REGN10987 in REGN-COV2, may enhance its overall efficacy against SARS-CoV-2.

Some research has found that antibodies do not retain significant activity against Omicron. For instance, the mAbs binding to escape the immune response is significantly weakened by the T478K, Q493K, Q498R, and E484A substitutions, especially in the case of etesevimab, bamlanivimab, sotrovimab, and CT-p59 (Shah & Woo, 2021). Additionally, Omicron may significantly reduce the effectiveness of the Eli Lilly antibody cocktail, and its potential to escape the vaccine is roughly twice as high as that of the Delta variant (Chen et al., 2022; Omotuyi et al., 2022).

One of the limitations of molecular dynamics simulations is the accuracy of current force fields and the challenge of conformational sampling. To address the conformational sampling issue, we recommend utilizing protein structures obtained through X-ray diffraction with a resolution of less than 3 Å. Additionally, to improve the accuracy of our simulations, it's advisable to assess various force fields such as AMBER (Tian et al., 2020) or CHARMM (J. Huang et al., 2017). However, we

are constrained to use the AMBER force field for our simulations due to current constraints. Furthermore, molecular dynamics simulations often encounter limitations in timescale exploration. If the results within the initial 100 nanoseconds exhibit instability, extending the simulation time becomes necessary for obtaining more reliable outcomes.

Conclusions

The RBD region plays a vital role in binding the virus to the host receptor, and mutations mainly occur in this region. Thus, this study focused on analyzing the RBD region's binding ability on the S protein with the ACE2 receptor and antibodies of the SARS-CoV-2 wild type, Delta variant, and Omicron variant. The results indicate that when binding to ACE2, Delta and Omicron variants had better binding ability, but these complexes were less stable over time than the wild type. The REGN10987 antibody could bind strongly with the Omicron variant while binding weakly with the Delta variant, suggesting its potential effectiveness against Omicron and ineffectiveness against Delta. Meanwhile, the REGN10933 antibody remains functional but exhibits a high risk of immune escape with Delta and Omicron variants. We suggest conducting continued experiments on the Delta and Omicron, as well as other prospective mutants, to confirm the binding ability of SARS-CoV-2 variants.

Authors' contributions

Conceptualization, Khac-Minh Thai; data curation, Thanh-Phuong Vo and Khac-Minh Thai; Formal analysis, Truong Lam Tuong, Dieu-Thuong Thi Trinh, Tan Thanh Mai, Quoc-Thai Nguyen, Thi-Thao-Nhung Nguyen, Thanh-Phuong Vo, Dac-Nhan Nguyen and Cong-Thanh Phan-Van; funding acquisition, Dieu-Thuong Thi Trinh, Quoc-Thai Nguyen and Khac-Minh Thai; investigation, Van-Thanh Tran, Dieu-Thuong Thi Trinh, Tan Thanh Mai, Quoc-Thai Nguyen, Thi-Thao-Nhung Nguyen, Thanh-Phuong Vo, Truong Lam Tuong, Dac-Nhan Nguyen and Cong-Thanh Phan-Van; methodology, Van-Thanh Tran, Dieu-Thuong Thi Trinh and Khac-Minh Thai; project administration, Dac-Nhan Nguyen and Khac-Minh Thai; resources, Van-Thanh Tran, Dieu-Thuong Thi Trinh, Tan Thanh Mai, Quoc-Thai Nguyen and Khac-Minh Thai; software, Tan Thanh Mai, Thanh-Phuong Vo, Dac-Nhan Nguyen and Khac-Minh Thai; supervision, Khac-Minh Thai; validation, Van-Thanh Tran, Dieu-Thuong Thi Trinh, Tan Thanh Mai, Quoc-Thai Nguyen, Thi-Thao-Nhung Nguyen, Dac-Nhan Nguyen and Khac-Minh Thai; visualization, Quoc-Thai Nguyen, Dac-Nhan Nguyen and Cong-Thanh Phan-Van; writing—original draft, Van-Thanh Tran, Truong Lam Tuong, Dieu-Thuong Thi Trinh, Tan Thanh Mai, Quoc-Thai Nguyen, Thi-Thao-Nhung Nguyen, Thanh-Phuong Vo, Dac-Nhan Nguyen, Cong-Thanh Phan-Van and Khac-Minh Thai; writing—review & editing, Van-Thanh Tran, Dac-Nhan Nguyen, Cong-Thanh Phan-Van and Khac-Minh Thai.

Disclosure statement

No potential conflict of interest was reported by the authors.

Funding

This research received no external funding.

ORCID

Quoc-Thai Nguyen  <http://orcid.org/0000-0001-6315-2974>
Khac-Minh Thai  <http://orcid.org/0000-0002-5279-9614>

References

- Barton, M. I., Macgowan, S., Kutuzov, M., Dushek, O., Barton, G. J., & Anton Van Der Merwe, P. (2021). Effects of common mutations in the SARS-CoV-2 spike RBD and its ligand the human ACE2 receptor on binding affinity and kinetics. *eLife*, 10, e70658. <https://doi.org/10.7554/eLife.70658>
- Bhardwaj, V. K., Singh, R., Sharma, J., Rajendran, V., Purohit, R., & Kumar, S. (2021). Identification of bioactive molecules from tea plant as SARS-CoV-2 main protease inhibitors. *Journal of Biomolecular Structure & Dynamics*, 39(10), 3449–3458. <https://doi.org/10.1080/07391102.2020.1766572>
- Bonvinlab. (2022). HADDOCK2.4 basic protein-protein docking tutorial. Bonvin & CSB Lab. <https://www.bonvinlab.org/education/HADDOCK24/HADDOCK24-protein-protein-basic/>
- Boonstra, S., Onck, P. R., & van der Giessen, E. (2016). CHARMM TIP3P water model suppresses peptide folding by solvating the unfolded state. *Journal of Physical Chemistry. B*, 120(15), 3692–3698. <https://doi.org/10.1021/acs.jpcc.6b01316>
- Bussi, G., Donadio, D., & Parrinello, M. (2007). Canonical sampling through velocity rescaling. *Journal of Chemical Physics*, 126(1), 014101. <https://doi.org/10.1063/1.2408420>
- Cao, Y., Wang, J., Jian, F., Xiao, T., Song, W., Yisimayi, A., Huang, W., Li, Q., Wang, P., An, R., Wang, J., Wang, Y., Niu, X., Yang, S., Liang, H., Sun, H., Li, T., Yu, Y., Cui, Q., & Xie, X. S. (2022). Omicron escapes the majority of existing SARS-CoV-2 neutralizing antibodies. *Nature*, 602(7898), 657–663. <https://doi.org/10.1038/s41586-021-04385-3>
- Chavda, V. P., Bezbaruah, R., Deka, K., Nongrang, L., & Kalita, T. (2022). The Delta and Omicron variants of SARS-CoV-2: What we know so far. *Vaccines*, 10(11), 1926. <https://doi.org/10.3390/vaccines10111926>
- Chen, J., Wang, R., Gilby, N. B., & Wei, G. W. (2022). Omicron variant (B.1.1.529): Infectivity, vaccine breakthrough, and antibody resistance. *Journal of Chemical Information and Modeling*, 62(2), 412–422. https://doi.org/10.1021/ACS.JCIM.1C01451/SUPPL_FILE/C1C01451_SI_002.PDF
- Cui, J., Li, F., & Shi, Z. L. (2019). Origin and evolution of pathogenic coronaviruses. *Nature Reviews Microbiology*, 17(3), 181–192. <https://doi.org/10.1038/s41579-018-0118-9>
- Deeks, E. D. (2021). Casirivimab/imdevimab: First approval. *Drugs*, 81(17), 2047–2055. <https://doi.org/10.1007/S40265-021-01620-Z>
- Dhama, K., Nainu, F., Frediansyah, A., Yatoo, M. I., Mohapatra, R. K., Chakraborty, S., Zhou, H., Islam, M. R., Mamada, S., Kusuma, H. I., Rabaan, A. A., Alhumaid, S., Mutair, A. A., Iqhrammullah, M., Al-Tawfiq, J. A., Mohaini, M. A., Alsaman, A. J., Tuli, H. S., Chakraborty, C., & Harapan, H. (2023). Global emerging Omicron variant of SARS-CoV-2: Impacts, challenges and strategies. *Journal of Infection and Public Health*, 16(1), 4–14. <https://doi.org/10.1016/j.jiph.2022.11.024>
- Durham, E., Dorris, B., Woetzel, N., Staritzbichler, R., & Meiler, J. (2009). Solvent accessible surface area approximations for rapid and accurate protein structure prediction. *Journal of Molecular Modeling*, 15(9), 1093–1108. <https://doi.org/10.1007/S00894-009-0454-9/TABLES/7>
- Ecdc. (2022). Implications of the emergence and spread of the SARS-CoV-2 variants of concern BA.4 and BA.5 for the EU/EEA. <https://epipulse.ecdc.europa.eu/ebs/#/item/details/2022->
- Gómez, J., Albaiceta, G. M., García-Clemente, M., López-Larrea, C., Amado-Rodríguez, L., Lopez-Alonso, I., Hermida, T., Enriquez, A. I., Herrero, P., Melón, S., Alvarez-Argüelles, M. E., Boga, J. A., Rojo-Alba, S., Cuesta-Llavona, E., Alvarez, V., Lorca, R., & Coto, E. (2020). Angiotensin-converting enzymes (ACE, ACE2) gene variants and COVID-19 outcome. *Gene*, 762, 145102. <https://doi.org/10.1016/J.GENE.2020.145102>
- GROMACS 2020.4 Manual. (n.d). <https://zenodo.org/records/4054996#.Y2MsUHZBy00>
- Han, P., Li, L., Liu, S., Wang, Q., Zhang, D., Xu, Z., Han, P., Li, XIA. O. MEI, Peng, Q., Su, C., Huang, B., Li, D., Zhang, R., Tian, M., Fu, L., Gao, Y., Zhao, X., Liu, K., Qi, J., Gao, G. F., & Wang, P. (2022). Receptor binding and complex structures of human ACE2 to spike RBD from omicron and delta SARS-CoV-2. *Cell*, 185(4), 630–640.e10. <https://doi.org/10.1016/J.CELL.2022.01.001>
- Hansen, J., Baum, A., Pascal, K. E., Russo, V., Giordano, S., Wloga, E., Fulton, B. O., Yan, Y., Koon, K., Patel, K., Chung, K. M., HeRMann, A., Ullman, E., Cruz, J., Rafique, A., Huang, T., Fairhurst, J., Libertiny, C., Malbec, M., & Kyrtasous, C. A. (2020). Studies in humanized mice and convalescent

- humans yield a SARS-CoV-2 antibody cocktail. *Science (New York, N.Y.)*, 369(6506), 1010–1014. https://doi.org/10.1126/SCIENCE.ABD0827/SUPPL_FILE/ABD0827_MJAR-REPRODUCIBILITYCHECKLIST.PDF
- Hoffmann, M., Kleine-Weber, H., Schroeder, S., Krüger, N., Herrler, T., Erichsen, S., Schiergens, T. S., Herrler, G., Wu, N. H., Nitsche, A., Müller, M. A., Drosten, C., & Pöhlmann, S. (2020). SARS-CoV-2 cell entry depends on ACE2 and TMPRSS2 and is blocked by a clinically proven protease inhibitor. *Cell*, 181(2), 271–280.e8. <https://doi.org/10.1016/j.cell.2020.02.052>
- Huang, J., Rauscher, S., Nawrocki, G., Ran, T., Feig, M., de Groot, B. L., Grubmüller, H., & MacKerell, A. D. (2017). CHARMM36m: An improved force field for folded and intrinsically disordered proteins. *Nature Methods*, 14(1), 71–73. <https://doi.org/10.1038/nmeth.4067>
- Huang, S.-Y. (2014). Search strategies and evaluation in protein–protein docking: Principles, advances and challenges. *Drug Discovery Today*, 19(8), 1081–1096. <https://doi.org/10.1016/j.drudis.2014.02.005>
- Iacob, S., & Iacob, D. G. (2020). SARS-CoV-2 treatment approaches: Numerous options, no certainty for a versatile virus. *Frontiers in Pharmacology*, 11, 1224. <https://doi.org/10.3389/fphar.2020.01224/BIBTEX>
- Islam, F., Dhawan, M., Nafady, M. H., Emran, T. B., Mitra, S., Choudhary, O. P., & Akter, A. (2022). Understanding the omicron variant (B.1.1.529) of SARS-CoV-2: Mutational impacts, concerns, and the possible solutions. *Annals of Medicine & Surgery*, 78. https://journals.lww.com/annals-of-medicine-and-surgery/fulltext/2022/06000/understanding_the_omicron_variant_b_1_1_529_of.39.aspx <https://doi.org/10.1016/j.amsu.2022.103737>
- Jackson, C. B., Farzan, M., Chen, B., & Choe, H. (2022). Mechanisms of SARS-CoV-2 entry into cells. *Nature Reviews. Molecular Cell Biology*, 23(1), 3–20. <https://doi.org/10.1038/s41580-021-00418-x>
- Jo, S., Cheng, X., Islam, S. M., Huang, L., Rui, H., Zhu, A., Lee, H. S., Qi, Y., Han, W., VANommeslaeghe, K., MacKerell, A. D., Roux, B., & Im, W. (2014). CHARMM-GUI PDB manipulator for advanced modeling and simulations of proteins containing nonstandard residues. *Advances in Protein Chemistry and Structural Biology*, 96, 235–265. <https://doi.org/10.1016/BS.APCSB.2014.06.002>
- Jo, S., Kim, T., Iyer, V. G., & Im, W. (2008). CHARMM-GUI: A web-based graphical user interface for CHARMM. *Journal of Computational Chemistry*, 29(11), 1859–1865. <https://doi.org/10.1002/JCC.20945>
- Kumar, S., Thambiraja, T. S., Karuppanan, K., & Subramaniam, G. (2022). Omicron and Delta variant of SARS-CoV-2: A comparative computational study of spike protein. *Journal of Medical Virology*, 94(4), 1641–1649. <https://doi.org/10.1002/JMV.27526>
- Lan, J., Ge, J., Yu, J., Shan, S., Zhou, H., Fan, S., Zhang, Q., Shi, X., Wang, Q., Zhang, L., & Wang, X. (2020). Structure of the SARS-CoV-2 spike receptor-binding domain bound to the ACE2 receptor. *Nature*, 581(7807), 215–220. <https://doi.org/10.1038/s41586-020-2180-5>
- Le, M.-T., Hoang, V.-N., Nguyen, D.-N., Bui, T.-H.-L., Phan, T.-V., Huynh, P. N., Tran, T.-D., & Thai, K.-M. (2021). Structure-based discovery of abcg2 inhibitors: A homology protein-based pharmacophore modeling and molecular docking approach. *Molecules (Basel, Switzerland)*, 26(11), 3115. <https://doi.org/10.3390/molecules26113115>
- Le, M.-T., Mai, T. T., Huynh, P. N. H., Tran, T.-D., Thai, K.-M., & Nguyen, Q.-T. (2020). Structure-based discovery of interleukin-33 inhibitors: A pharmacophore modelling, molecular docking, and molecular dynamics simulation approach. *SAR and QSAR in Environmental Research*, 31(12), 883–904. <https://doi.org/10.1080/1062936X.2020.1837239>
- Liu, Y., Liu, J., Plante, K. S., Plante, J. A., Xie, X., Zhang, X., Ku, Z., An, Z., Scharton, D., Schindewolf, C., Widen, S. G., Menachery, V. D., Shi, P.-Y., & Weaver, S. C. (2022). The N501Y spike substitution enhances SARS-CoV-2 infection and transmission. *Nature*, 602(7896), 294–299. <https://doi.org/10.1038/s41586-021-04245-0>
- Mahase, E. (2020). Covid-19: RECOVERY trial will evaluate antiviral antibody cocktail. *BMJ (Clinical Research ed.)*, 370, m3584. <https://doi.org/10.1136/BMJ.M3584>
- Mai, T. T., Nguyen, P. G., Le, M.-T., Tran, T.-D., Huynh, P. N. H., Trinh, D.-T. T., Nguyen, Q.-T., & Thai, K.-M. (2022). Discovery of small molecular inhibitors for interleukin-33/ST2 protein–protein interaction: A virtual screening, molecular dynamics simulations and binding free energy calculations. *Molecular Diversity*, 26(5), 2659–2678. <https://doi.org/10.1007/s11030-021-10359-4>
- Möhlendick, B., Schönfelder, K., Breuckmann, K., Elsner, C., Babel, N., Balfanz, P., Dahl, E., Dreher, M., Fistera, D., Herbstreit, F., Hölzer, B., Koch, M., Kohnle, M., Marx, N., Risse, J., Schmidt, K., Skrzypczyk, S., Sutharsan, S., Taube, C., & Kribben, A. N. DREAS (2021). ACE2 polymorphism and susceptibility for SARS-CoV-2 infection and severity of COVID-19. *Pharmacogenetics and Genomics*, 31(8), 165–171. <https://doi.org/10.1097/FPC.0000000000000436>
- Omotuyi, O., Olubiyi, O., Nash, O., Afolabi, E., Oyinloye, B., Fatumo, S., Femi-Oyewo, M., & BOGoro, S. (2022). SARS-CoV-2 Omicron spike glycoprotein receptor binding domain exhibits super-binder ability with ACE2 but not convalescent monoclonal antibody. *Computers in Biology and Medicine*, 142, 105226. <https://doi.org/10.1016/J.COMPBIOMED.2022.105226>
- Park, S.-J., Kern, N., Brown, T., Lee, J., & Im, W. (2023). CHARMM-GUI PDB manipulator: Various PDB structural modifications for biomolecular modeling and simulation. *Journal of Molecular Biology*, 435(14), 167995. <https://doi.org/10.1016/j.jmb.2023.167995>
- Parrinello, M., & Rahman, A. (1981). Polymorphic transitions in single crystals: A new molecular dynamics method. *Journal of Applied Physics*, 52(12), 7182–7190. <https://doi.org/10.1063/1.328693>
- Phan, T.-V., Nguyen, V.-T.-V., Le, M.-T., Nguyen, B. G. D., Vu, T.-T., & Thai, K.-M. (2024). Identification of efflux pump inhibitors for *Pseudomonas aeruginosa* MexAB-OprM via ligand-based pharmacophores, 2D-QSAR, molecular docking, and molecular dynamics approaches. *Molecular Diversity*, 28(5), 3295–3311. <https://doi.org/10.1007/s11030-023-10758-9>
- Phan, T.-V., Nguyen, V.-T.-V., Nguyen, C.-H.-H., Vu, T.-T., Tran, T.-D., Le, M.-T., Trinh, D.-T. T., Tran, V.-H., & Thai, K.-M. (2023). Discovery of AcrAB-TolC pump inhibitors: Virtual screening and molecular dynamics simulation approach. *Journal of Biomolecular Structure & Dynamics*, 41(22), 12503–12520. <https://doi.org/10.1080/07391102.2023.2175381>
- Phan, T.-V., Tuong, L.-T., Nguyen, V.-T.-V., Vo, C.-V. T., Tran, T.-D., Le, M.-T., Nguyen, B. G. D., Tran, V.-T., Vu, T.-T., & Thai, K.-M. (2023). Computational assessment and in vitro test of phytochemicals of *Usnea aciculifera* as potential inhibitors of *Escherichia coli* efflux pump AcrB. *Journal of Biomolecular Structure & Dynamics*, 1–13. <https://doi.org/10.1080/07391102.2023.2291547>
- Planas, D., Veyer, D., Baidaliuk, A., Staropoli, I., Guivel-Benhassine, F., Rajah, M. M., Planchais, C., Porrot, F., Robillard, N., Puech, J., Prot, M., Gallais, F., Gantner, P., Velay, A., Le Guen, J., Kassis-Chikhani, N., Edriss, D., Belec, L., Seve, A., & Schwartz, O. (2021). Reduced sensitivity of SARS-CoV-2 variant Delta to antibody neutralization. *Nature*, 596(7871), 276–280. <https://doi.org/10.1038/s41586-021-03777-9>
- Premkumar, L., Segovia-Chumbez, B., Jadhav, R., Martinez, D. R., Raut, R. A. JENDRA, Markmann, A., Cornaby, C., Bartelt, L., Weiss, S., Park, Y., Edwards, C. T. L. E., Weimer, E., Scherer, E. M., Roupheal, N., Edupuganti, S., Weiskopf, D., Tse, L. V., Hou, Y. J., Margolis, D., & de Silva, A. M. (2020). The receptor-binding domain of the viral spike protein is an immunodominant and highly specific target of antibodies in SARS-CoV-2 patients. *Science Immunology*, 5(48), eabc8413. <https://doi.org/10.1126/SCIIMMUNOL.ABC8413>
- Regeneron Pharmaceuticals. (2020). *Regeneron's casirivimab and imdevimab antibody cocktail for COVID-19 is first combination therapy to receive FDA emergency use authorization*. www.regeneron.com
- Regeneron Pharmaceuticals. (2023). *Safety, tolerability, and efficacy of anti-spike (S) SARS-CoV-2 monoclonal antibodies for hospitalized adult patients with COVID-19*. ClinicalTrials.gov, National Library of Medicine. SARS-CoV-2 Variants of Concern as of 12 April 2024. (n.d). <https://www.ecdc.europa.eu/en/covid-19/variants-concern>
- Shah, M., & Woo, H. G. (2021). Omicron: A heavily mutated SARS-CoV-2 variant exhibits stronger binding to ACE2 and potentially escapes approved COVID-19 therapeutic antibodies. *Frontiers in Immunology*, 12, 830527. <https://doi.org/10.3389/FIMMU.2021.830527/BIBTEX>
- Sharma, J., Kumar Bhardwaj, V., Singh, R., Rajendran, V., Purohit, R., & Kumar, S. (2021). An in-silico evaluation of different bioactive molecules of tea for their inhibition potency against non structural protein-15 of SARS-CoV-2. *Food Chemistry*, 346, 128933. <https://doi.org/10.1016/j.foodchem.2020.128933>
- Singh, R., & Purohit, R. (2024). Multi-target approach against SARS-CoV-2 by stone apple molecules: A master key to drug design. *Phytotherapy Research: PTR*, 38(1), 7–10. <https://doi.org/10.1002/ptr.7772>

- Singh, R., Bhardwaj, V. K., Sharma, J., Kumar, D., & Purohit, R. (2021). Identification of potential plant bioactive as SARS-CoV-2 spike protein and human ACE2 fusion inhibitors. *Computers in Biology and Medicine*, 136, 104631. <https://doi.org/10.1016/j.compbiomed.2021.104631>
- Sundar, S., Thangamani, L., Manivel, G., Kumar, P., & Piramanayagam, S. (2019). Molecular docking, molecular dynamics and MM/PBSA studies of FDA approved drugs for protein kinase a of *Mycobacterium tuberculosis*: Application insights of drug repurposing. *Informatics in Medicine Unlocked*, 16, 100210. <https://doi.org/10.1016/j.imu.2019.100210>
- Suzuki, R., Yamasoba, D., Kimura, I., Wang, L., Kishimoto, M., Ito, J., Morioka, Y., Nao, N., Nasser, H., Uriu, K., Kosugi, Y., Tsuda, M., Orba, Y. A. SUKO., Sasaki, M., Shimizu, R., KAWabata, R., Yoshimatsu, K., Asakura, H., Nagashima, M., & Sato, K. Genotype to Phenotype Japan (G2P-Japan) Consortium. (2022). Attenuated fusogenicity and pathogenicity of SARS-CoV-2 Omicron variant. *Nature*, 603(7902), 700–705. <https://doi.org/10.1038/s41586-022-04462-1>
- Tada, T., Zhou, H., Dcosta, B. M., Samanovic, M. I., Mulligan, M. J., & Landau, N. R. (2021). Partial resistance of SARS-CoV-2 Delta variants to vaccine-elicited antibodies and convalescent sera. *iScience*, 24(11), 103341. <https://doi.org/10.1016/j.iisci.2021.103341>
- Takashita, E., Kinoshita, N., Yamayoshi, S., Sakai-Tagawa, Y., Fujisaki, S., Ito, M., Iwatsuki-Horimoto, K., Chiba, S., Halfmann, P., Nagai, H., Saito, M. A. KOTO., Adachi, E., Sullivan, D., Pekosz, A., Watanabe, S., Maeda, K., Imai, M. A. SAKI., Yotsuyanagi, H., Mitsuya, H., & Kawaoka, Y. O. SHIHIRO (2022). Efficacy of antibodies and antiviral drugs against Covid-19 Omicron variant. *New England Journal of Medicine*, 386(10), 995–998. <https://doi.org/10.1056/NEJMC2119407>
- Tandel, D., Gupta, D., Sah, V., & Harshan, K. H. (2021). N440K variant of SARS-CoV-2 has higher infectious fitness. *BioRxiv*. <https://doi.org/10.1101/2021.04.30.441434>
- Thai, K.-M., Le, D.-P., Tran, N.-V.-K., Nguyen, T.-T.-H., Tran, T.-D., & Le, M.-T. (2015). Computational assay of Zanamivir binding affinity with original and mutant influenza neuraminidase 9 using molecular docking. *Journal of Theoretical Biology*, 385, 31–39. <https://doi.org/10.1016/j.jtbi.2015.08.019>
- Tian, C., Kasavajhala, K., Belfon, K. A. A., Raguette, L., Huang, H., Migues, A. N., Bickel, J., Wang, Y., Pincay, J., Wu, Q., & Simmerling, C. (2020). ff19SB: Amino-acid-specific protein backbone parameters trained against quantum mechanics energy surfaces in solution. *Journal of Chemical Theory and Computation*, 16(1), 528–552. <https://doi.org/10.1021/acs.jctc.9b00591>
- Tracking SARS-CoV-2 Variants. (n.d). <https://www.who.int/activities/tracking-SARS-CoV-2-variants>
- Tran, Q.-H., Cao, H.-N., Nguyen, D.-N., Tran, T.-T.-N., Le, M.-T., Nguyen, Q.-T., Tran, V.-T., Tran, V.-H., & Thai, K.-M. (2023). Targeting olokizumab-interleukin 6 interaction interface to discover novel IL-6 inhibitors. *Journal of Biomolecular Structure & Dynamics*, 41(23), 14003–14015. <https://doi.org/10.1080/07391102.2023.2193990>
- Tran, T.-T.-N., Tran, Q.-H., Duong, C. Q., Nguyen, Q.-T., Tran, V.-T., Le, M.-T., Tran, V.-H., & Thai, K.-M. (2023). In silico approach to identify novel allosteric intracellular antagonist for blocking the interleukin-8/CXCR2 receptor signaling pathway. *Journal of Biomolecular Structure & Dynamics*, 41(22), 13154–13167. <https://doi.org/10.1080/07391102.2023.2171136>
- Tran, V.-T., Tran, V.-H., Nguyen, D.-N., Do, T.-G.-S., Vo, T.-P., Nguyen, T.-T.-N., Huynh, P. N. H., & Thai, K.-M. (2022). The effects of one-point mutation on the New Delhi metallo beta-lactamase-1 resistance toward carbapenem antibiotics and β -lactamase inhibitors: An in silico systematic approach. *International Journal of Molecular Sciences*, 23(24), 16083. <https://doi.org/10.3390/ijms232416083>
- Tran-Nguyen, V. K., Le, M. T., Tran, T. D., Truong, V. D., & Thai, K. M. (2019). Peramivir binding affinity with influenza A neuraminidase and research on its mutations using an induced-fit docking approach. *SAR and QSAR in Environmental Research*, 30(12), 899–917. <https://doi.org/10.1080/1062936X.2019.1679248>
- Tuccori, M., Ferraro, S., Convertino, I., Cappello, E., Valdiserra, G., Blandizzi, C., Maggi, F., & Focosi, D. (2020). Anti-SARS-CoV-2 neutralizing monoclonal antibodies: Clinical pipeline. *mAbs*, 12(1), 1854149. <https://doi.org/10.1080/19420862.2020.1854149>
- Vakser, I. A. (2014). Protein-protein docking: From interaction to interactome. *Biophysical Journal*, 107(8), 1785–1793. <https://doi.org/10.1016/j.bpj.2014.08.033>
- Van Zundert, G. C. P., Rodrigues, J. P. G. L. M., Trellet, M., Schmitz, C., Kastiris, P. L., Karaca, E., Melquiond, A. S. J., Van Dijk, M., De Vries, S. J., & Bonvin, A. M. J. J. (2016). The HADDOCK2.2 web server: User-friendly integrative modeling of biomolecular complexes. *Journal of Molecular Biology*, 428(4), 720–725. <https://doi.org/10.1016/J.JMB.2015.09.014>
- Vangone, A., Rodrigues, J. P. G. L. M., Xue, L. C., van Zundert, G. C. P., Geng, C., Kurkcuoglu, Z., Nellen, M., Narasimhan, S., Karaca, E., van Dijk, M., Melquiond, A. S. J., Visscher, K. M., Trellet, M., Kastiris, P. L., & Bonvin, A. M. J. J. (2017). Sense and simplicity in HADDOCK scoring: Lessons from CASP-CAPRI round 1. *Proteins*, 85(3), 417–423. <https://doi.org/10.1002/prot.25198>
- Variants of the Virus. (2023). *Centers for disease control and prevention*.
- Walls, A. C., Park, Y. J., Tortorici, M. A., Wall, A., McGuire, A. T., & Veeler, D. (2020). Structure, function, and antigenicity of the SARS-CoV-2 spike glycoprotein. *Cell*, 181(2), 281–292.e6. <https://doi.org/10.1016/J.CELL.2020.02.058/ATTACHMENT/OD452E6C-56C8-4028-8AFB-CFC22B1A37FF/MMC2.PDF>
- Wang, Q., Zhang, Y., Wu, L., Niu, S., Song, C., Zhang, Z., Lu, G., Qiao, C., Hu, Y., Yuen, K. Y., Wang, Q., Zhou, H., Yan, J., & Qi, J. (2020). Structural and functional basis of SARS-CoV-2 entry by using human ACE2. *Cell*, 181(4), 894–904.e9. <https://doi.org/10.1016/J.CELL.2020.03.045>
- World Health Organization. (2024a). Number of COVID-19 cases reported to WHO (cumulative total) – World. <https://data.who.int/dashboards/covid19/cases?n=o>
- World Health Organization. (2024b). Number of COVID-19 deaths reported to WHO (cumulative total) – World. <https://data.who.int/dashboards/covid19/deaths?n=o>
- Wrapp, D., Wang, N., Corbett, K. S., Goldsmith, J. A., Hsieh, C.-L., Abiona, O., Graham, B. S., & McLellan, J. S. (2020). Cryo-EM structure of the 2019-nCoV spike in the prefusion conformation. *Science (New York, N.Y.)*, 367(6483), 1260–1263. <https://doi.org/10.1126/science.abb2507>
- Xiao, W., Wang, D., Shen, Z., Li, S., & Li, H. (2018). Multi-body interactions in molecular docking program devised with key water molecules in protein binding sites. *Molecules (Basel, Switzerland)*, 23(9), 2321. <https://doi.org/10.3390/MOLECULES23092321>
- Xue, L. C., Rodrigues, J. P., Kastiris, P. L., Bonvin, A. M., & Vangone, A. (2016). PRODIGY: A web server for predicting the binding affinity of protein-protein complexes. *Bioinformatics (Oxford, England)*, 32(23), 3676–3678. <https://doi.org/10.1093/BIOINFORMATICS/BTW514>
- Yang, J., Petitjean, S. J. L., Koehler, M., Zhang, Q., Dumitru, A. C., Chen, W., Derclaye, S., ViNCent, S. P., Soumilion, P., & Alsteens, D. (2020). Molecular interaction and inhibition of SARS-CoV-2 binding to the ACE2 receptor. *Nature Communications*, 11(1), 4541. <https://doi.org/10.1038/s41467-020-18319-6>
- Zhou, P., Yang, X.-L., Wang, X.-G., Hu, B., Zhang, L., Zhang, W., Si, H.-R., Zhu, Y., Li, B., Huang, C.-L., Chen, H.-D., Chen, J., Luo, Y., Guo, H., Jiang, R.-D., Liu, M.-Q., Chen, Y., Shen, X.-R., Wang, X., & Shi, Z.-L. (2020). A pneumonia outbreak associated with a new coronavirus of probable bat origin. *Nature*, 579(7798), 270–273. <https://doi.org/10.1038/s41586-020-2012-7>